https://doi.org/10.5194/egusphere-2023-1727
Preprint. Discussion started: 18 September 2023

Technical Note: Analytical Solution for Well Water Response to Earth Tides in Leaky Aquifers with Storage and Compressibility in the Aquitard

Rémi Valois[1, 2, *], Agnès Rivière[3], Jean-Michel Vouillamoz[4], Gabriel C. Rau[5]

[1]French Red-Cross, 4 rue Diderot, Paris, France
[2]Hydrogeology Lab, UMR EMMAH, University of Avignon, 74 rue Louis Pasteur, Avignon, France
[3]Geosciences Department, Mines Paris - PSL, 75272 Paris, France
[4]Univ. Grenoble Alpes, IRD, CNRS, INRAE, Grenoble INP, IGE, 38000 Grenoble, France
[5]School of Environmental and Life Sciences, The University of Newcastle, Callaghan, Australia

*Correspondence: remi.valois1@gmail.com; Tel.: +33-6-8434-0779 (R.V.)

Key points

- Development of a new analytical solution for Earth tide induced well water level fluctuations in semi-confined aquifers considering aquitard storage, aquitard response to tidal strain, skin and wellbore storage effects
- The solution correctly reflects previously observed but unexplained amplitude-frequency relationships and positive or negative phase shifts
- Diagnostic information about subsurface hydro-geomechanical properties can be derived from amplitude ratio and phase shifts for both semi-diurnal and diurnal tides

Abstract

In recent years, there has been a growing interest in utilizing the groundwater response to Earth tides as a means to estimate subsurface properties. However, existing analytical models have been insufficient in accurately capturing realistic physical conditions. This study presents a new analytical solution to calculate groundwater response to Earth tide strains, including storage and compressibility of the aquitard, borehole storage and skin effects. We investigate the effects of aquifer and aquitard parameters on well water response to Earth tides at two dominant frequencies (O_1 and M_2) and compare our results with hydraulic parameters obtained from a pumping test. Inversion of the six hydro-geomechanical parameters from amplitude response and phase shift of both semi-diurnal and diurnal tides provides relevant information about aquifer transmissivity, storativity, well skin effect, aquitard hydraulic conductivity and diffusivity. The new model is able to reproduce previously unexplained observations of the amplitude and frequency responses. We emphasize the usefulness in developing relevant methodology to use the groundwater response to natural drivers for characterizing hydrogeological systems.

https://doi.org/10.5194/egusphere-2023-1727
Preprint. Discussion started: 18 September 2023

1. Introduction

Aquifer properties play a vital role in managing groundwater resources, particularly amid increasing anthropogenic groundwater use and the impact of climate change. While pump testing can be costly, there exists a cost-effective alternative for assessing aquifer hydraulic properties - analysing the groundwater response to Earth tides or atmospheric tides (McMillan et al., 2019). Observations of variations in groundwater level due to tidal fluctuations date back to the works of Klönne (1880), Meinzer (1939), and Young (1913). However, it was only later that hydro-geomechanical models were employed to elucidate these variations (Bredehoeft, 1967; Hsieh and Bredehoeft, 1987; Roeloffs, 1996; Wang, 2000; Cutillo and Bredehoeft, 2011; Kitagawa et al., 2011; Lai et al., 2013; Wang et al., 2018). This progression in understanding offers a valuable opportunity to evaluate aquifer hydraulic properties through the response of groundwater to tidal fluctuations.

Hsieh and Bredehoeft (1987) introduced the horizontal flow model, focusing on confined conditions influenced by tidal forces. Conversely, Roeloffs (1996) and Wang (2000) explored interactions within vertical flow under tidal fluctuations. Wang et al. (2018) expanded on these studies by incorporating a flow from an upper aquitard, albeit assuming negligible storage within it. Later, Gao et al. (2020) extended these models to include borehole skin effects. Thomas et al. (2023) developed an ET-GW model incorporating storage and strain response in the aquitard. They applied their model to a specific site to evaluate transmissivity variations and validated it using pumping tests.

Numerous studies have investigated aquifer hydromechanical properties by analysing GW level variations induced by Earth tides, employing the models mentioned in the previous literature (Narasimhan et al., 1984; Merritt, 2004; Fuentes-Arreazola et al., 2018; Zhang et al., 2019a; Shen et al., 2020). However, only a limited number of validations have been conducted, which involve comparing the results with robust hydraulic assessments, such as hydraulic conductivity derived from slug testing (Zhang et al., 2019b) or specific storage and transmissivity characterizations obtained through long-term pumping tests (Allègre et al., 2016; Valois et al., 2022). The current evaluations predominantly focus on purely confined conditions, leaving a gap in knowledge regarding tidally induced GW responses in aquifers under semi-confined conditions.

As far as the authors are aware, the publications by Sun et al. (2020), Valois et al. (2022), and Thomas et al. (2023) are the sole references addressing a comparison for a leaky aquifer. Sun et al. (2020) found significant discrepancies between transmissivities obtained from Earth tide fluctuations and those derived from slug or pump tests. However, it is worth noting that the comparison may be subject to discussion, as the authors employed a leaky aquifer model for analysing tidally induced fluctuations, whereas they used a confined aquifer model for conducting slug and pump tests. In the study conducted by Valois et al. (2022), the existing Earth-Tide GroundWater (ET-GW) models, as described

https://doi.org/10.5194/egusphere-2023-1727
Preprint. Discussion started: 18 September 2023

earlier, were unable to reproduce a low semi-diurnal to diurnal amplitude ratio with positive phase shifts in conjunction with pumping test transmissivity data. This discrepancy highlights the complexity and challenges in modelling tidally induced groundwater responses in leaky aquifers and the need for further investigation in this area.

We note that our previous attempts to model the observed substantial amplitude decrease from O_1 to M_2 frequency, combined with phase shifts close to zero, proved unsuccessful when using Earth tide models found in the literature. None of the existing models could provide satisfactory results. The pursuit of an explanation led to the realisation that analytical solutions with more realistic assumptions are required. For example, aquifers are widely recognized to be influenced by aquitards, which often consist of highly porous and compressible clay materials, contributing significant amounts of stored water to the aquifer (Moench, 1985). Moreover, these aquitards are also impacted by Earth tide strains (Bastias et al., 2022).

Our first objective is to develop an analytical solution considering storage and strain in the aquitard. Unlike Thomas et al. (2023), our model incorporates borehole skin effects and allows for a fixed hydraulic head at the top of the aquitard, broadening its applicability to a broader range of hydrogeological conditions. The second motivation of our study is to develop a model that better fits the observed results by considering aquitard storage, as evident in the pumping tests. Third, we compare the results obtained from our new ET-GW model with those derived from a pumping test in leaky aquifers with storage in the aquitard. Fourth, since most publications have predominantly focused on assessing hydraulic properties using the semi-diurnal tide (M_2), our third motivation is to demonstrate the potential of using diurnal tides (O_1) in combination with the semi-diurnal (M_2 or N_2) to provide a more comprehensive characterization of aquifer and aquitard hydro-mechanical properties. Our new development offers the potential to enhance hydraulic and geomechanical subsurface characterization by employing a more realistic model for the groundwater response to natural forces.

2. Groundwater response to Earth tides in a leaky aquifer with aquitard storage and strain

Hantush (1960) pioneered the modelling of aquitard storage by modifying the leaky aquifer theory to account for storage in the aquitard. In our study, we consider a semi-confined configuration (Figure 1) where the target aquifer is overlain by an aquitard that allows for storage, strain, and vertical flux. Both layers are assumed to be slightly compressible, spatially homogenous, infinite laterally, and have constant thickness. Building upon the work of Wang et al. (2018), our research incorporates Earth Tide

(ET) fluctuations into the leaky aquifer equations proposed by Moench (1985). Additionally, we incorporate the skin effect, as described by Gao et al. (2020).

Groundwater flow and storage in an aquifer overlain by an aquitard can be described as:

$$T\left(\frac{\partial^2 h}{\partial r^2}+\frac{1}{r}\frac{\partial h}{\partial r}\right)=S\left(\frac{\partial h}{\partial t}-\frac{BK_u}{\rho g}\frac{\partial \varepsilon}{\partial t}\right)-K'\frac{\partial h'}{\partial z} \quad (1)$$

$$\left(\frac{\partial^2 h'}{\partial z^2}\right)=\frac{1}{D'}\left(\frac{\partial h'}{\partial t}-\frac{B'K'_u}{\rho g}\frac{\partial \varepsilon}{\partial t}\right) \quad . \quad (2)$$

Here, h (m) and h' (m) are the hydraulic heads in the aquifer and the aquitard respectively; h'_j (m) is the fixed hydraulic head at the top of the aquitard, r (m) is the radial distance from the studied well; T (m²/s) and S are the aquifer transmissivity and storativity; B, B', K_u (Pa), K'_u (Pa) are the Skempton's coefficient and the undrained bulk modulus of the aquifer and aquitard respectively; ρ (kg/m^3) and g (m/s²) are the water density and gravity constant; ε is the volumetric Earth tide strain; K' (m/s) is the aquitard hydraulic conductivity; S_s' (m^{-1}) is the specific storage of the aquitard; D' (m²/s) is aquitard hydraulic diffusivity (K'/S_s' ratio). Any natural regional groundwater flow is considered negligible.

Borehole drilling causes a zone of damage with a radius r_s (see Figure 1) that is responsible for the skin effect (Van Everdingen, 1953). A negative skin can be caused by a greater hydraulic conductivity around the well because of the material damaged by the drilling, while a positive skin can be associated by porosity clogging caused by the drilling mud. This is reflected in the well's pressure head Δh_s. The skin factor (sk) can be defined as:

$$sk=\frac{\Delta h_s}{\left(r\frac{\partial h}{\partial r}\right)_{r=r_w}} \quad . \quad (3)$$

Following above assumptions, the boundary conditions are

$$h(r,t)=h_\infty(t)\ at\ r=\infty \quad (4)$$

$$h_w(t)=h(r,t)-sk\left(r\frac{\partial h(r,t)}{\partial r}\right)\ at\ r=r_w \quad (5)$$

$$2\pi r_w T\left(\frac{\partial h}{\partial r}\right)_{r=r_w}=\pi r_c^2\frac{\partial h_w}{\partial t} \quad (6)$$

$$h'=h\ at\ z=z_i \quad . \quad (7)$$

$$h'=h'_j\ at\ z=0 \quad (8)$$

Here, t is the time (s); r_w and r_c are the radius of the well screened portion and the radius of well casing in which water level fluctuates; z_i is the aquifer-aquitard interface elevation (see Figure 1) and h_w is the hydraulic head at r_w.

https://doi.org/10.5194/egusphere-2023-1727
Preprint. Discussion started: 18 September 2023

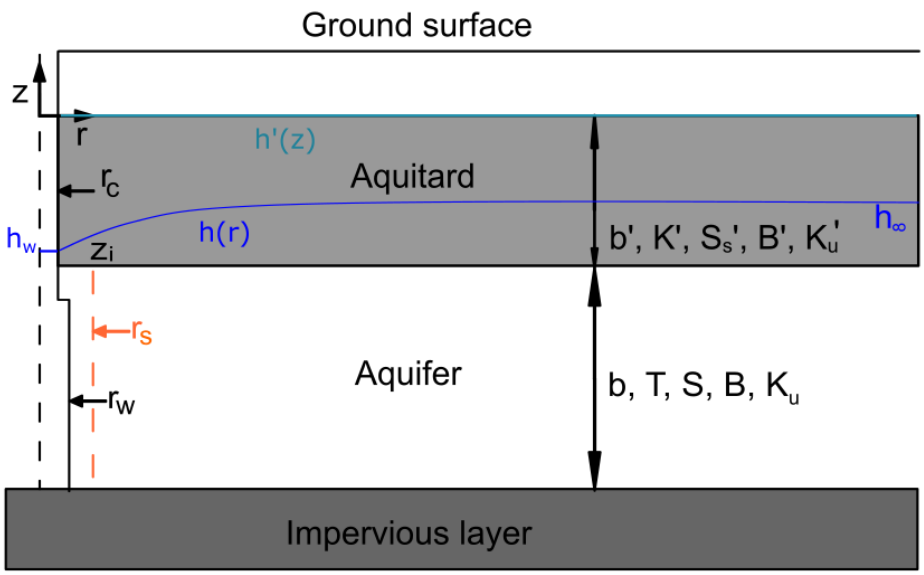

Figure 1: Semi-confined system with a compressible aquitard with storage

Following Hsieh et al. (1987) and Wang et al. (2018), complex numbers were used to facilitate harmonic model development and the solution is obtained by first solving Equation 2 in the aquitard, then deriving the head response in the aquifer far away from the well (h_∞) which is independent of the radial distance. Then, the well effect on the aquifer response is considered by using a flux condition at the well that accounts for wellbore storage. Since h', h, ε, h_w, h_∞ are all periodic functions, they can be expressed as:

$$\varepsilon(t) = \varepsilon_0 e^{i\omega t} \tag{9}$$

$$h_\infty(t) = h_{\infty,0} e^{i\omega t} \tag{10}$$

$$h_w(t) = h_{w,0} e^{i\omega t} \tag{11}$$

$$h(r,t) = h_0(r) e^{i\omega t} \tag{12}$$

$$h'(z,t) = h_0'(z) e^{i\omega t} \quad . \tag{13}$$

Here, $i = \sqrt{-1}$; ε_0 (m) is the ET strain amplitude and ω (s[-1]) is the angular frequency. In this case, Equation 2 becomes:

$$\left(\frac{\partial^2 h_0'}{\partial z^2}\right) = \frac{1}{D\prime}\left(i\omega h_0' - i\omega \frac{B\prime K_u'}{\rho g} \varepsilon_0\right) \quad . \tag{14}$$

According to Wang (2000) and Roeloffs (1996) and as detailed in appendix A, the solution of Equation 2 is:

$$h'_0 = A_1 e^{\frac{(1+i)}{\delta}(z-z_i)} + A_2 e^{-\frac{(1+i)}{\delta}(z-z_i)} + \frac{B'K'_u}{\rho g}\varepsilon_0 \qquad (15)$$

where $\delta = \left(\frac{2D'}{\omega}\right)^{1/2}$. Thus, at the interface between the aquifer and the aquitard (z=z_i), we have pressure continuity as $h'(z_i,t) = h_0 e^{i\omega t} = h(t)$ which leads to:

$$\left(\frac{\partial h'}{\partial z}\right)_{z=z_i} = \frac{1+i}{\delta}\left(\frac{h_0 - \frac{B'K'_u}{\rho g}\varepsilon_0}{\tanh\left(\frac{1+i}{\delta}z_i\right)} - \frac{h'_j - \frac{B'K'_u}{\rho g}\varepsilon_0}{\sinh\left(\frac{1+i}{\delta}z_i\right)}\right) e^{i\omega t} \quad . \qquad (16)$$

Equation 1 can be solved far away from the well using h_∞ which is independent of the radial distance from the well and by using the source term from h' as follows

$$0 = \frac{\partial h_\infty}{\partial t} - \frac{BK_u}{\rho g}\frac{\partial \varepsilon}{\partial t} - \frac{K'}{S}\frac{1+i}{\delta}\left(\frac{h_\infty - \frac{B'K'_u}{\rho g}\varepsilon_0}{\tanh\left(\frac{1+i}{\delta}z_i\right)} - \frac{h'_j - \frac{B'K'_u}{\rho g}\varepsilon_0}{\sinh\left(\frac{1+i}{\delta}z_i\right)}\right) e^{i\omega t} \qquad (17)$$

$$h_{\infty,0} = \frac{BK_u}{\rho g}\varepsilon_0 \frac{Si\omega + K'\frac{1+i}{\delta}\frac{B'K'_u}{BK_u}\left(\frac{-1}{\tanh\left(\frac{1+i}{\delta}z_i\right)} - \frac{h'_j\frac{\rho g}{B'K'_u\varepsilon_0} - 1}{\sinh\left(\frac{1+i}{\delta}z_i\right)}\right)}{Si\omega - K'\frac{1+i}{\delta}\frac{1}{\tanh\left(\frac{1+i}{\delta}z_i\right)}} \quad . \qquad (18)$$

The disturbance in water level due to the well can be expressed as:

$$s(r,t) = h(r,t) - h_\infty(t) \quad . \qquad (19)$$

Equation 1 becomes:

$$T\left(\frac{\partial^2 s}{\partial r^2} + \frac{1}{r}\frac{\partial s}{\partial r}\right) = S\left(\frac{\partial s}{\partial t}\right) - K'\frac{1+i}{\delta}s\frac{1}{\tanh\left(\frac{1+i}{\delta}z_i\right)} \qquad (20)$$

with the boundary conditions:

$$s(r \to \infty) = 0 \qquad (21)$$

$$h_{w,0} - h_{\infty,0} = s - sk\left(r\frac{\partial s}{\partial r}\right) \qquad at\ r = r_w \qquad (22)$$

$$2\pi r_w T\left(\frac{\partial s}{\partial r}\right)_{r=r_w} = i\omega\pi r_c^2 h_{w,0} \quad . \qquad (23)$$

The solution of this differential equation is $s(r) = C_I I_0(\beta r) + C_K K_0(\beta r)$ (Wang *et al.*, 2018), where I_0 and K_0 are the modified Bessel functions of the first and second kind and the zeroth order, respectively. Further,

https://doi.org/10.5194/egusphere-2023-1727
Preprint. Discussion started: 18 September 2023

$$\beta = \left(\frac{i\omega S}{T} - \frac{K\prime}{T}\frac{(1+i)}{\delta}\frac{1}{\tanh\left(\frac{1+i}{\delta}z_i\right)}\right)^{1/2} \quad . \qquad (24)$$

The boundary conditions lead to C_l=0 and $C_K = -\frac{i\omega r_c^2 h_{w,0}}{2T\beta r_w K_1(\beta r_w)}$ because $\frac{dK_0(r)}{dr} = -K_1(r)$. Therefore, the final solution for the well water level is:

$$h_{w,0} = \frac{BK_u}{\rho g}\varepsilon_0 \frac{Si\omega + K'\frac{1+i}{\delta}\frac{B'K_u'}{BK_u}\left(\frac{-1}{\tanh\left(\frac{1+i}{\delta}z_i\right)} - \frac{h_j'\frac{\rho g}{B'K_u'\varepsilon_0} - 1}{\sinh\left(\frac{1+i}{\delta}z_i\right)}\right)}{\sigma\left(Si\omega - K'\frac{1+i}{\delta}\frac{1}{\tanh\left(\frac{1+i}{\delta}z_i\right)}\right)} \quad , \qquad (25)$$

where

$$\sigma = 1 + \frac{i\omega r_c^2 K_0(\beta r_w)}{2T\beta r_w K_1(\beta r_w)} + \frac{i\omega r_c^2}{2T} sk \, . \qquad (26)$$

By assuming $h_j' = 0$ (i.e. the hydraulic head at the top of the aquitard corresponds to the unsaturated-saturated interface at z=0), Equation 25 can be reorganized to

$$h_{w,0} = \frac{BK_u}{\rho g}\varepsilon_0 \frac{Si\omega + K'\frac{1+i}{\delta}R_{KuB}\left(\frac{1-\cosh\left(\frac{1+i}{\delta}z_i\right)}{\sinh\left(\frac{1+i}{\delta}z_i\right)}\right)}{\sigma\left(Si\omega - K'\frac{1+i}{\delta}\frac{1}{\tanh\left(\frac{1+i}{\delta}z_i\right)}\right)} \quad , \qquad (27)$$

where

$$R_{KuB} = \frac{K_u'B'}{K_uB} \quad . \qquad (28)$$

By disregarding $\frac{BK_u}{\rho g}$ product which only controls the amplitude, the solution has six independent parameters which are *T*, *S*, *K'*, *D'*, *sk* and the R_{KuB} ratio.

Let us now define the amplitude response (or amplitude ratio), *A*, and phase shift, *α*, of the GW response to ET fluctuations:

$$A = \left| h_{w,0} / \frac{BK_u}{\rho g}\varepsilon_0 \right| \qquad (29)$$

$$\alpha = arg\left[h_{w,0} / \frac{BK_u}{\rho g}\varepsilon_0 \right] . \qquad (30)$$

Figure 2 shows the amplitude response and phase shift as a function of frequency using our new solution in comparison to key models reported in the literature. Aquitard parameters were set accoring to Batlle-Aguilar et al. (2016), while aquifer parameters were chosen accoring to the field application below. We validate the solution using a very low aquitard conductivity (10^{-14} m/s), so that we can

https://doi.org/10.5194/egusphere-2023-1727
Preprint. Discussion started: 18 September 2023

compare it to the horizontal flux with wellbore storage model (Hsieh et al., 1987). It shows a perfect match.

Because both horizontal and vertical flux models are associated with opposite phase shift signs (Figure 2b), the latter can offer valuable insights for model selection (Allègre et al., 2014). Positive phase shifts in the vertical flux model are related to an increasing amplitude ratio with frequency, whereas the wellbore storage model exhibits the opposite behaviour. Wang et al. (2018) developed a leaky model capable of demonstrating both positive and negative phase shifts, where positive phase shifts correspond to an increasing amplitude ratio with frequencies, and negative phase shifts are linked to a decreasing amplitude ratio.

Our new model showcases positive or negative phase shifts with an increasing or decreasing amplitude ratio over frequency, even allowing for amplitude ratios greater than one. Notably, Wang (2000) observed a similar characteristic in the vertical flux model, with an amplitude just above one (1.06) for very specific conditions. At high frequencies, our model displays amplitude ratios and phase shifts similar to those of the leaky and wellbore storage models, reflecting the attenuation of high-frequency pore pressure fluctuations in the aquifer by well water.

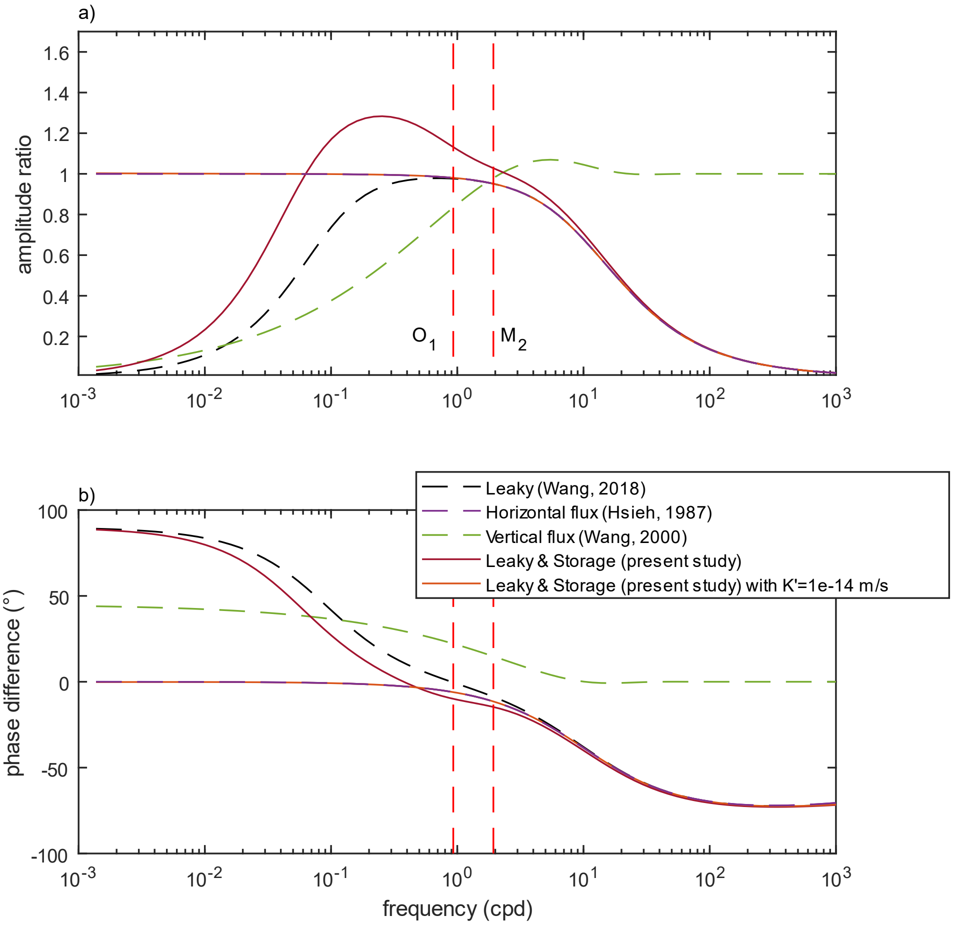

Figure 2: Frequency variation of amplitude response and phase shift of the groundwater response to Earth tides. The transmissivity (T) is 10^{-5} m²/s, storativity (S) is 10^{-4}, hydraulic conductivity of the aquitard (K') is 10^{-8} m/s, aquitard hydraulic diffusivity (D') is 10^{-4} m²/s, skin factor (sk) is 0, R_{KuB} to 1.4, well casing radius (r_c) and screen radius (r_w) is 6.03 cm. b' was set to 5 m. Screen depth (z) was set to 23 m for the vertical flow model of Wang (2000).

We explored the parameter space by focussing on the frequency-dependant amplitude response and phase shift responses for different sets of parameter values. The reference parameter set is the one described above. *T*, R_{KuB} and z_i have a large impact on model shapes. As also observed by Hsieh et al. (1987), *S* does not have a major impact on the results (Fig3c and 3d). The skin effect does not play a large role in the useful frequency band for amplitudes, but its influence is larger for the phase shifts when compared to the reference parameter set. *K'* does not significantly influence the results with

https://doi.org/10.5194/egusphere-2023-1727
Preprint. Discussion started: 18 September 2023

respect to the reference parameter set used in the study (Figures 3e to 3f). *K'* has the opposite role of *S* and they appear to compensate each others effects, because of their respective role in Equation 27.

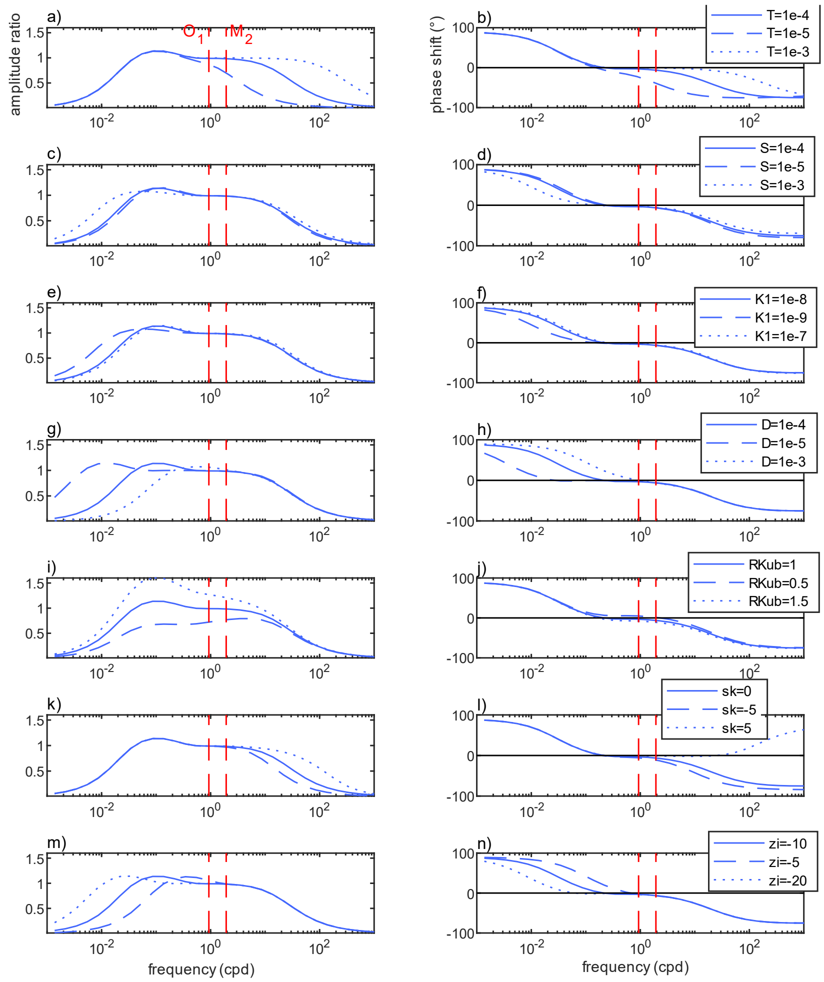

Figure 3: Illustration of the amplitude response (left column) and phase shift (right column) as a function of frequency for various parameters compared to the reference parameter set.

https://doi.org/10.5194/egusphere-2023-1727
Preprint. Discussion started: 18 September 2023

3. Application of the new model to a groundwater monitoring dataset from Cambodia

3.1 Field site and previous results

The field site in Northwest Cambodia comprises three boreholes drilled into the subsurface, consisting of mudstone, claystone, siltstone, and sandstone. Time series and pumping test results have been reported in Valois et al. (2022), while details of the lithology can be found in Vouillamoz et al. (2012; 2016) and Valois et al. (2017; 2018; 2022). Pumping from the aquifer is limited by a very low specific yield, attributed to the presence of fine deposits such as clay and mudstone (Vouillamoz et al. 2012; Valois et al., 2018).

The boreholes were drilled to a depth of 31 meters with a radius of 6 inches and equipped with 4-inch PVC casing from top to bottom, featuring a 9-meter long screen at the hole's base. The aquifer is situated within a hard rock media, comprising either claystone or sandstone, located beneath a 10-meter thick clay layer.

For the pumping tests, the wells were pumped for three days, and water levels were allowed to recover for four days in two observation wells. The interpretation of the pumping tests utilized AQTESOLV™/Pro v4.5 software, employing the leaky aquifer with aquitard storage model (Moench, 1985) or a 3D flow using the generalized radial flow model (Barker, 1988). The selected solutions, compared to other models (Theiss, Hantush without aquitard storage), demonstrated the best fit with a Root Mean Square Error (RMSE) of 0.02 m for Cambodia.

3.2 Well sensitivities and phase shifts to Earth tides

Between 2010 and 2015, well water levels were measured at 20, 40, or 60-minute intervals using absolute pressure sensors (Diver data loggers, Eijkelkamp Soil & Water, NL). To compensate for barometric pressure (BP) effects, data from a barometer located a few kilometres away from the field site were utilized (Eijkelkamp Soil & Water, NL). A zero-phase Butterworth filter was employed to eliminate low-frequency content (periods longer than 10 days) from both groundwater (GW) and BP data.

For each site's geolocation (latitude, longitude, and height), ET strain time series were computed at 20-minute intervals using SPOTL software (Agnew, 2012). The time series were then modelled using Harmonic Least-Squares (HALS; Schweizer et al., 2021) with eight frequencies corresponding to the major tides (Table 1) following Merritt's description (2004). HALS provides amplitude and phase estimations for each tidal component and record.

https://doi.org/10.5194/egusphere-2023-1727
Preprint. Discussion started: 18 September 2023

Table 1. *Dominant tidal components that are generally found in groundwater measurements (adapted from MacMillan et al., 2019)*

Darwin Name	Frequency (cpd)	Attribution
Q_1	0.89365	Earth
O_1	0.929536	Earth
P_1-	0.997262	Earth
S_1	1.000000	Atmosphere
K_1	1.002738	Earth
N_2	1.895982	Earth
M_2	1.932274	Earth
S_2	2.000000	Earth/Atmosphere
K_2	2.005476	Earth

The results obtained from HALS were utilized to calculate the amplitude response and phase shift between groundwater (GW) and Earth tide (ET) for each tidal component. These amplitude responses are commonly known as "well sensitivities" to Earth tide strains (Rojstaczer and Agnew, 1989) and are summarized in Figure 4 alongside the corresponding phase shifts.

The well sensitivities to tides exhibit a frequency-dependent behaviour, resulting in similar values for neighbouring frequencies and a generally decreasing magnitude. The amplitudes of M_2 and N_2 are relatively straightforward to assess due to their significant magnitudes (11.2 and 2.1 mm, respectively), and their amplitude responses and phase shifts are highly similar. The phase shifts for the tides of interest (O_1, N_2, and M_2) are positive. However, the signs of the amplitudes for the other tides can be attributed to their low amplitude responses, which are challenging to characterize using HALS.

https://doi.org/10.5194/egusphere-2023-1727
Preprint. Discussion started: 18 September 2023

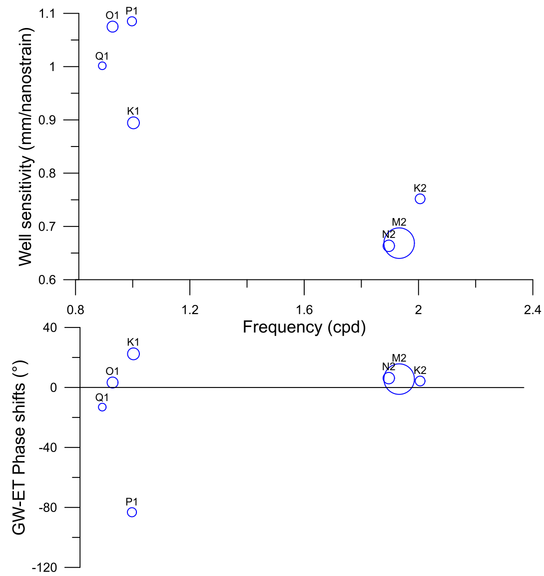

Figure 4: Amplitude responses and phase shifts as a function of frequency for the Cambodian site. S1 and S2 were excluded as they are not only generated by Earth tides. The circle size is proportional to the amplitude in the well water levels.

3.3 Fitting the M_2/O_1 amplitude response ratio and phase shifts

The analysis is restricted to two types of tides: the semi-diurnal and diurnal tides. This limitation arises because the magnitude of Earth tide-induced well water levels is significantly damped for higher frequencies, making it difficult to discern and analyse tides beyond these two types. Here, we use amplitude responses (A_{M2}, A_{O1}) and phase shifts (α_{M2}, α_{O1}) to estimate hydraulic subsurface properties. N_2 tide was not used since its response may be too similar to M_2 and does not help with constraining the model. Amplitudes are influenced by geomechanical parameters (BK_u) which are generally not considered in classical hydrogeology. Valois et al. (2022) previously illustrated that the M_2 to O_1 amplitude response ratio can be computed because it is not directly multiplied by BK_u and because it provides useful information about model choice. This leads to a system of three equations and six parameters (T, S, K', D', *skin*, and R_{KuB}) by using the simplified model in Equation 27 when the geometry of the well and the aquitard-aquifer system is known:

$$\frac{A_{M2}}{A_{O1}} = \left|h_{w,0,\omega=M_2} / h_{w,0,\omega=O_2}\right| \tag{31}$$

$$\alpha_{M2} = arg\left[h_{w,0,\omega=M_2} / \frac{BK_u}{\rho g}\varepsilon_0\right] \tag{32}$$

$$\alpha_{O1} = arg\left[h_{w,0,\omega=O_1} / \frac{BK_u}{\rho g}\varepsilon_0\right]. \tag{33}$$

Table 2 displays the data to be fitted using the three equations above.

https://doi.org/10.5194/egusphere-2023-1727
Preprint. Discussion started: 18 September 2023

Table 2: Data to be fitted using the ET-GW model

	$\frac{A_{M2}}{A_{O1}}$	α_{M2} (°)	α_{O1} (°)
Cambodia	0.62	5.62	3.3

A systematic exploration of the entire parameter space without any constraints other than the well and aquifer geometry was carried out. Hydraulic and geomechanical property ranges are chosen according to the literature, i.e., De Marsily (1986) and Domenico and Schwartz (1998). In order to assess the goodness of fit with the three observed parameters (Eqs 31 to 33), the objective chi-square function is defined below:

$$\chi^2 = {}^1/_N \sum_{i=1}^{N} \left(\frac{(Obs_i - Mod_i)}{Error_i}\right)^2 \quad (34)$$

where *N* is the number of observed parameters (3 here), Obs_i, Mod_i and $Error_i$ are the observed parameter, modeled parameter and their errors respectively. Thus, this objective function takes into account errors of the observed parameters (De Pasquale et al.; 2022). They were set to 0.1°, 0.5° and 0.2 for α_{M2}, α_{O1} and $\frac{A_{M2}}{A_{O1}}$ respectively, according to Valois et al. (2022).

The model allows to fit both O_1 and M_2 positive phases and the low M_2 to O_1 amplitude ratio (misfit closed to 0 in Fig. 5), whereas the model of Gao et al (2020) cannot (misfit above 1 see Appendix B, and Valois et al., 2020). The *T* value is in good agreement with the pumping test range (Fig. 5a). *S* is half an order of magnitude below the pumping test range (Fig 5b) whereas the storativity best-fit for Gao et al (2020) is two orders of magnitude above (Appendix B). The skin effect also shows acceptable values as compared to the pumping test (Fig 5f). The parameter exploration shows best-fits for *K'* and *D'*, whereas it is difficult to identify a clear best-fit for the R_{KuB} parameter. The values are within the expected range for the hydrogeological configuration: The mudstone aquitard has a lower hydraulic conductivity (10^{-8} m/s) than the underlying claystone aquifer (coarser grain size than the aquitard, with a *K* value of about 10^{-7} m/s for an aquifer thickness of 22 m), and a diffusivity of about 10^{-4} m²/s. This is in agreement with the aquitard classification of Pacheco (2013).

https://doi.org/10.5194/egusphere-2023-1727
Preprint. Discussion started: 18 September 2023

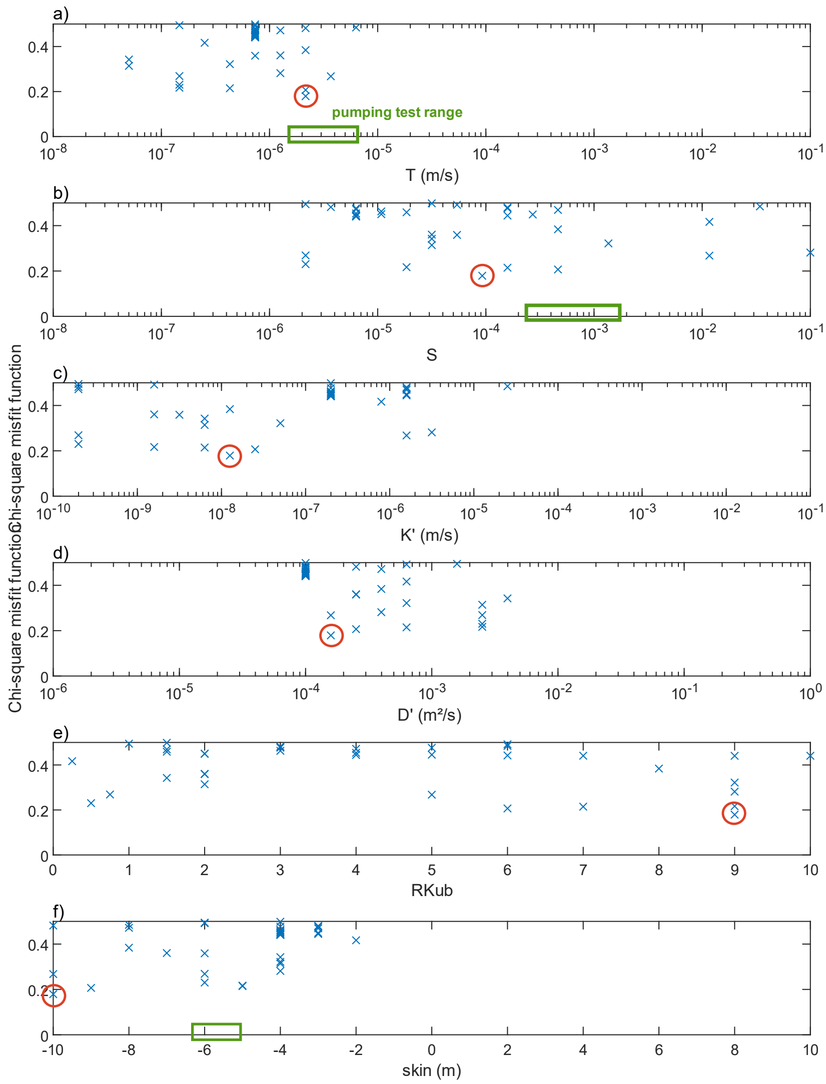

Figure 5: Results of full parameters exploration using two leaky aquifer models for the Cambodian case study.

4. DISCUSSION

4.1. Uncertainties and discrepancies

There are several sources of uncertainty which originate from measurement and their propagation as well as uncertainties introduced by model assumptions. We believe that uncertainties linked to pressure sensor resolution (0.2 mm) and time resolution (20 minutes) as well as the HALS

https://doi.org/10.5194/egusphere-2023-1727
Preprint. Discussion started: 18 September 2023

decomposition were too low to be worth considering, at least for the semi-diurnal tides. This can be deduced from the nearly identical amplitude responses at M_2 and N_2 at our field site. Because those responses are indeed identical, it means that errors in the raw data set did not influence the response characterization. We note that amplitude responses and phase shifts show larger discrepancies for the diurnal tides. This could be linked to overall lower amplitudes which are generally more difficult to characterise. We therefore conclude that errors arising from uncertainties are negligible compared to the uncertainty introduced by model assumptions, in agreement with Sun *et al.* (2020).

Discrepancies between hydro-geomechanical properties derived from the groundwater response to Earth tides (termed as "passive" and assuming a compressible matrix) and hydraulic testing (e.g., slug, pump and lab testing, termed as "active" and generally assuming an incompressible matrix) have been reported in the literature and have not been appropriately reconciled. By fitting amplitude response ratio and phase shifts (Section 3.3), a T value discrepancy of one order of magnitude can be observed between both approaches. We hypothesise that this is caused by parameter anisotropy.

Zhang *et al.* (2019b) pointed out differences in hydraulic conductivities of more than one order of magnitude between ET analysis and slug tests and attributed this to differences in the investigated scale. Allègre *et al.* (2016) reported much higher values of storativity derived from pumping test is compared to ET when using the vertical flow model. Sun *et al.* (2020) showed that T values are frequency-dependent with several orders of magnitude differences when comparing co-seismic, ET, slug or pump test methods. The discrepancies can be explained by the different conceptual models used in the active (based on perfectly confined) and passive methods (based on leaky conditions) or by the frequency dependency of hydraulic parameters. The literature illustrates that transmissivity, hydraulic conductivity or specific storage can indeed vary depending on the frequency of the forcing (e.g., Cartwright *et al.,* 2005; Renner and Messar, 2006; Guiltinan and Becker, 2015; Rabinovich *et al.,* 2015). This demonstrates the need for attention when assessing hydraulic parameters using passive methods for semi-confined conditions. We specifically emphasise the need for using the same conceptual model (i.e., confined, leaky with or without storage, vertical flow) when comparing active and passive methods, as well as the need of preliminary hydrogeological knowledge of both the aquifer system (i.e., presence of an aquitard with or without storage) (Bastias et al., 2022) as well as the borehole skin effect.

4.2. The use of the leaky model with aquitard storage

Our new analytical solution describing the well water level response to harmonic Earth tide strains contains at least six hydro-geomechanical parameters that could be derived from only three features, e.g., M_2 to O_1 amplitude response ratio and M_2 and O_1 phase shifts. Applying this model to real-world

https://doi.org/10.5194/egusphere-2023-1727
Preprint. Discussion started: 18 September 2023

cases to derive properties from amplitude responses and phase shifts provides relevant information on *T*, *S*, *D*′, *K*′, and skin effect, but it is prone to non-uniqueness. Thus, a priori information may be needed depending on the capacity of the inverse problem to fit observed data (phases shifts and amplitude ratio). In our case study, parameter assessment would benefit from prior information on *S* (or *K*′) and R_{KuB}.

The model presented in this study can be useful when the hydrogeological configuration involves storage in the aquitard with fixed head (i.e., Dirichlet) boundary conditions and for cases where phase shifts and amplitude ratio do exemplify a specific pattern. For example, when compared to Gao et al (2020) and using the parametrisation of the present study (Fig. 6), our solution is able to model lower M_2 to O_1 amplitude ratio, lower phases, and higher amplitude ratio for phases closed to 0.

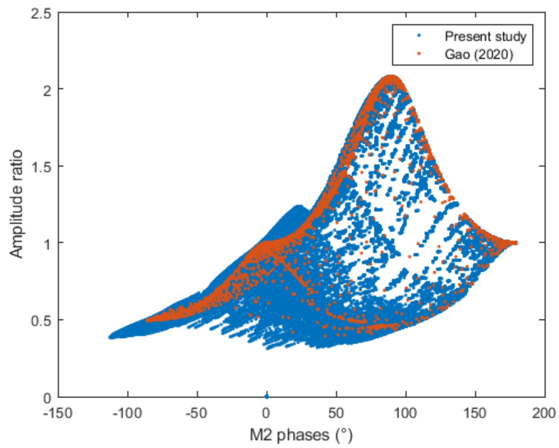

Figure 6: Outputs of the models using the parametrization of the study (rc=rw=6.08 cm, z_i=-10 m).

While the amplitudes are controlled by the product of the Skempton coefficient and the undrained bulk modulus, these mechanical parameters also affect phase shifts. Therefore, further investigations are needed to assess these influences using other methods or to link them empirically with the hydraulic parameters. This is crucial to enhance confidence in utilizing groundwater response to Earth tides as a valuable tool for better understanding and characterizing groundwater resources.

5. Conclusion

We have developed a new analytical solution for the well water level response to Earth tide strains. This solution considers a previously unprecedented physical reality, specifically, a leaky aquifer with

https://doi.org/10.5194/egusphere-2023-1727
Preprint. Discussion started: 18 September 2023

aquitard storage, subject to Dirichlet boundary conditions under tidal strain. Additionally, our model considers the influence of borehole storage and skin effects, further improving the accuracy and comprehensiveness of the analysis. This model extends upon previous models and allows advanced characterization of the subsurface using the groundwater response to natural forces. The new model overcomes previous limitations, for example it explains very low M_2 to O_1 amplitude ratios as well as large phase shift difference between M_2 and O_1 tides. The model relies on six combinations of hydro-geomechanical parameters. In this study, we assess the most sensitive parameters to be the transmissivity, the well skin effect, the aquitard to aquifer mechanical parameters ratio ($B'K_u'/BK_u$), as well as aquitard diffusivity and aquitard conductivity to aquifer storativity ratio.

We apply our new model to a groundwater monitoring dataset from Cambodia and compare the results with pumping tests undertaken in the same formation. We used the diurnal (O_1) and semi-diurnal (M_2) tides to better constrain the model. Results illustrate significant insight into subsurface properties. For example, we derive relevant information about T, S, D', K', and *skin effect*, when compared to the pumping test results. Overall, our new model can be used to shed light on previously inexplicable well water level behaviour and can be paired with other investigation methods to enhance understanding of subsurface processes.

Competing interests

The contact author has declared that none of the authors has any competing interests.

Acknowledgements

This work has been carried out in the framework of the Institut de Recherche pour le Développement and the French Red Cross collaborative project 39842A1 - 1R012-RHYD, with the financial support of the European Community (grant DIPECHO SEA ECHO/DIP/BUD/2010/01017 and grant DCI-FOOD/2011/278-175).

References

Agnew, D. C. (2012), SPOTL: Some programs for ocean-tide loading, SIO technical report, Scripps Institution of Oceanography, UC San Diego, Calif. [Available at http://escholarship.org/uc/sio_techreport.]

Allègre, V., Brodsky, E. E., Xue, L., Nale, S. M., Parker, B. L., & Cherry, J. A. (2016). Using earth-tide induced water pressure changes to measure in situ permeability: A comparison with long-term pumping tests. *Water Resources Research*, *52*(4), 3113-3126.

https://doi.org/10.5194/egusphere-2023-1727
Preprint. Discussion started: 18 September 2023

Barker, J. A. (1988). A generalized radial flow model for hydraulic tests in fractured rock. Water Resources Research, 24(10), 1796-1804.

Bastias Espejo, J. M., Rau, G. C., & Blum, P. (2022). Groundwater responses to Earth tides: Evaluation of analytical solutions using numerical simulation. Journal of Geophysical Research: Solid Earth, 127, e2022JB024771. https://doi.org/10.1029/2022JB024771

Batlle-Aguilar, J., Cook, P.G., Harrington, G.A., 2016. Comparison of hydraulic and chemical methods for determining hydraulic conductivity and leakage rates in argillaceous aquitards. J. Hydrol. 532, 102–121. https://doi.org/10.1016/j.jhydrol.2015.11.035

Bredehoeft, J. D. (1967). Response of well-aquifer systems to earth tides. *Journal of Geophysical Research*, *72*(12), 3075-3087.

De Marsily G (1986) Quantitative hydrogeology. Academic, San Diego, CA.

De Pasquale, G., Valois, R., Schaffer, N., & MacDonell, S. (2022). Contrasting geophysical signatures of a relict and an intact Andean rock glacier. The Cryosphere, 16(5), 1579-1596.

Domenico PA, Schwartz FW (1998) Physical and chemical hydrogeology, 2nd edn. Wiley, Chichester, UK.

Cartwright, N., Nielsen, P., & Perrochet, P. (2005). Influence of capillarity on a simple harmonic oscillating water table: Sand column experiments and modeling. *Water resources research*, *41*(8).Cutillo, P. A., &Bredehoeft, J. D. (2011). Estimating aquifer properties from the water level response to Earth tides. *Groundwater*, *49*(4), 600-610.

Fuentes-Arreazola, M. A., Ramírez-Hernández, J., & Vázquez-González, R. (2018). Hydrogeological properties estimation from groundwater level natural fluctuations analysis as a low-cost tool for the Mexicali Valley Aquifer. *Water*, *10*(5), 586.

Gao, X., Sato, K., & Horne, R. N. (2020). General Solution for Tidal Behavior in Confined and Semiconfined Aquifers Considering Skin and Wellbore Storage Effects. *Water Resources Research*, 56(6), e2020WR027195.

Guiltinan, E., & Becker, M. W. (2015). Measuring well hydraulic connectivity in fractured bedrock using periodic slug tests. *Journal of Hydrology*, *521*, 100-107.

Hantush, M. S. (1960). Modification of the theory of leaky aquifers. Journal of Geophysical Research, 65(11), 3713-3725.

Hsieh, P. A., Bredehoeft, J. D., & Farr, J. M. (1987). Determination of aquifer transmissivity from Earth tide analysis. *Water resources research*, *23*(10), 1824-1832.

Kitagawa, Y., Itaba, S., Matsumoto, N., & Koizumi, N. (2011). Frequency characteristics of the response of water pressure in a closed well to volumetric strain in the high-frequency domain. *Journal of Geophysical Research: Solid Earth*, *116*(B8).https://doi.org/10.1029/2010JB007794

Klonne, F. W. (1880). Die periodischenschwankungen des wasserspiegels in den inundietenkohlenschachten von Dux in der period von 8 April bis 15 September 1879 (The periodic fluctuations of water levels in the flooded coal mine at Dux in the period 8 April to 15 September 1879). SitzungsberichteKaiserliche Akademie der Wissenschaften in Wien.

Kuang, X., Jiao, J. J., Zheng, C., Cherry, J. A., & Li, H. (2020). A review of specific storage in aquifers. *Journal of Hydrology*, *581*, 124383.

Lai, G., Ge, H., & Wang, W. (2013). Transfer functions of the well-aquifer systems response to atmospheric loading and Earth tide from low to high-frequency band. *Journal of Geophysical Research: Solid Earth*, *118*(5), 1904-1924.

McMillan, T. C., Rau, G. C., Timms, W. A., & Andersen, M. S. (2019). Utilizing the impact of Earth and atmospheric tides on groundwater systems: A review reveals the future potential. *Reviews of Geophysics*, *57*(2), 281-315.

Meinzer, O. E. (1939). Ground water in the United States, a summary of ground-water conditions and resources, utilization of water from wells and springs, methods of scientific investigation, and literature relating to the subject, (Tech. Rep. 1938-39). U.S. Department of the Interior, Geological Survey. https://doi.org/10.3133/wsp836D

Melchior, P. (1983). The tides of the planet Earth. *Oxford*.

Merritt, M. L. (2004). *Estimating hydraulic properties of the Floridan aquifer system by analysis of earth-tide, ocean-tide, and barometric effects, Collier and Hendry Counties, Florida* (No. 3). US Department of the Interior, US Geological Survey.

Moench, A. F. (1985). Transient flow to a large-diameter well in an aquifer with storative semiconfining layers. Water Resources Research, 21(8), 1121-1131.

Narasimhan, T. N., Kanehiro, B. Y., & Witherspoon, P. A. (1984). Interpretation of earth tide response of three deep, confined aquifers. *Journal of Geophysical Research: Solid Earth*, *89*(B3), 1913-1924.

Pacheco, F. A. L. (2013). Hydraulic diffusivity and macrodispersivity calculations embedded in a geographic information system. Hydrological sciences journal, 58(4), 930-944.

Rabinovich, A., Barrash, W., Cardiff, M., Hochstetler, D. Ls., Bakhos, T., Dagan, G., &Kitanidis, P. K. (2015). Frequency dependent hydraulic properties estimated from oscillatory pumping tests in an unconfined aquifer. *Journal of Hydrology*, *531*, 2-16.

Renner, J., &Messar, M. (2006). Periodic pumping tests. *Geophysical Journal International*, *167*(1), 479-493.

Roeloffs, E. (1996). Poroelastic techniques in the study of earthquake-related hydrologic phenomena. *Advances in geophysics,* 37, 135-195. https://doi.org/10.1016/S0065-2687(08)60270-8

Rojstaczer, S., & Agnew, D. C. (1989). The influence of formation material properties on the response of water levels in wells to Earth tides and atmospheric loading. Journal of Geophysical Research: Solid Earth, 94(B9), 12403-12411.

Schweizer, D., Ried, V., Rau, G. C., Tuck, J. E., & Stoica, P. (2021). Comparing Methods and Defining Practical Requirements for Extracting Harmonic Tidal Components from Groundwater Level Measurements. *Mathematical Geosciences*, 1-23.

Shen, Q., Zheming, S., Guangcai, W., Qingyu, X., Zejun, Z., &Jiaqian, H. (2020). Using water-level fluctuations in response to Earth-tide and barometric-pressure changes to measure the in-situ hydrogeological properties of an overburden aquifer in a coalfield. *Hydrogeology Journal*, 1-15.

Sun, X., Shi, Z., Xiang, Y (2020). Frequency dependence of in-situ transmissivity estimation of well-aquifer systems from periodic loadings. *Water Resources Research*, e2020WR027536.

Valois, R., Vouillamoz, J. M., Lun, S., &Arnout, L. (2017). Assessment of water resources to support the development of irrigation in northwest Cambodia: a water budget approach. *Hydrological Sciences Journal*, *62*(11), 1840-1855.

Valois, R., Vouillamoz, J. M., Lun, S., &Arnout, L. (2018). Mapping groundwater reserves in northwestern Cambodia with the combined use of data from lithologs and time-domain-electromagnetic and magnetic-resonance soundings. *Hydrogeology Journal*, *26*(4), 1187-1200.

Valois, R., Rau, G. C., Vouillamoz, J. M., & Derode, B. (2022). Estimating hydraulic properties of the shallow subsurface using the groundwater response to Earth and atmospheric tides: a comparison with pumping tests. *Water Resources Research*, *58*(5), e2021WR031666.

Van Everdingen, A. F. (1953). The skin effect and its influence on the productive capacity of a well. *Journal of petroleum technology*, *5*(06), 171-176.

Vouillamoz, J. M., Sokheng, S., Bruyere, O., Caron, D., &Arnout, L. (2012). Towards a better estimate of storage properties of aquifer with magnetic resonance sounding. *Journal of Hydrology*, *458*, 51-58.

Vouillamoz, J. M., Valois, R., Lun, S., Caron, D., &Arnout, L. (2016). Can groundwater secure drinking-water supply and supplementary irrigation in new settlements of North-West Cambodia? *Hydrogeology Journal*, *24*(1), 195-209.

Wang, C. Y., Doan, M. L., Xue, L., & Barbour, A. J. (2018). Tidal response of groundwater in a leaky aquifer—Application to Oklahoma. *Water Resources Research*, *54*(10), 8019-8033.https://doi.org/10.1029/2018WR022793

Wang, H. F. (2000). *Theory of linear poroelasticity with applications to geomechanics and hydrogeology* (Vol. 2). Princeton University Press.

Young, A. (1913). Tidal phenomena at inland boreholes near Cradock. *Transactions of the Royal Society of South Africa*, *3*(1), 61-106.

https://doi.org/10.5194/egusphere-2023-1727
Preprint. Discussion started: 18 September 2023

Zhang, H., Shi, Z., Wang, G., Sun, X., Yan, R., & Liu, C. (2019a). Large earthquake reshapes the groundwater flow system: Insight from the water-level response to earth tides and atmospheric pressure in a deep well. *Water Resources Research*, *55*(5), 4207-4219.

Zhang, S., Shi, Z., & Wang, G. (2019b). Comparison of aquifer parameters inferred from water level changes induced by slug test, earth tide and earthquake–A case study in the three Gorges area. *Journal of Hydrology*, *579*, 124169.

https://doi.org/10.5194/egusphere-2023-1727
Preprint. Discussion started: 18 September 2023

Appendix

Appendix A: The analytical solution in the aquitard

To solve Equation 14 with the boundary conditions in Equations 7 and 8, we define:

$$\widehat{h_0'} = h_0' - \frac{B'K_u'}{\rho g}\varepsilon_0 \qquad \text{(A1)}$$

Thus, the equation system become:

$$\left(\frac{\partial^2 \widehat{h_0'}}{\partial z^2}\right) = \frac{i\omega \widehat{h_0'}}{D'} \qquad \text{(A2)}$$

$$\widehat{h_0'}(z = z_i) = h_0 - \frac{B'K_u'}{\rho g}\varepsilon_0 \qquad \text{(A3)}$$

$$\widehat{h_0'}(z = 0) = h_j' - \frac{B'K_u'}{\rho g}\varepsilon_0 \qquad \text{(A4)}$$

The solution $\widehat{h_0'}$ is of the form:

$$\widehat{h_0'} = A_1 \mathrm{e}^{\frac{(1+i)}{\delta}(z-z_i)} + A_2 \mathrm{e}^{-\frac{(1+i)}{\delta}(z-z_i)} \qquad \text{(A5)}$$

It yields

$$A_1 = \frac{\mathrm{e}^{\frac{(1+i)}{\delta}z_i}\left(h_0 - \frac{B'K_u'}{\rho g}\varepsilon_0\right) - \left(h_j' - \frac{B'K_u'}{\rho g}\varepsilon_0\right)}{2\sinh\left(\frac{(1+i)}{\delta}z_i\right)} \qquad \text{(A6)}$$

$$A_2 = \frac{-\mathrm{e}^{-\frac{(1+i)}{\delta}z_i}\left(h_0 - \frac{B'K_u'}{\rho g}\varepsilon_0\right) + \left(h_j' - \frac{B'K_u'}{\rho g}\varepsilon_0\right)}{2\sinh\left(\frac{(1+i)}{\delta}z_i\right)} \qquad \text{(A7)}$$

Thus:

$$h_0' = A_1 \mathrm{e}^{\frac{(1+i)}{\delta}(z-z_i)} + A_2 \mathrm{e}^{-\frac{(1+i)}{\delta}(z-z_i)} + \frac{B'K_u'}{\rho g}\varepsilon_0 \qquad \text{(A8)}$$

Appendix B: Additional information on parameter exploration

The figure A1 shows the misfit functions using the model developed in this study and the model of Gao et al . (2020). Misfits are clearly higher for the older model that do not consider storage and tidal response in the aquitard. Storativity best-fit using the model of Gao et al (2020) failed to reproduce pumping test values. Nevertheless, transmissivity and skin estimates fall within pumping test range.

https://doi.org/10.5194/egusphere-2023-1727
Preprint. Discussion started: 18 September 2023

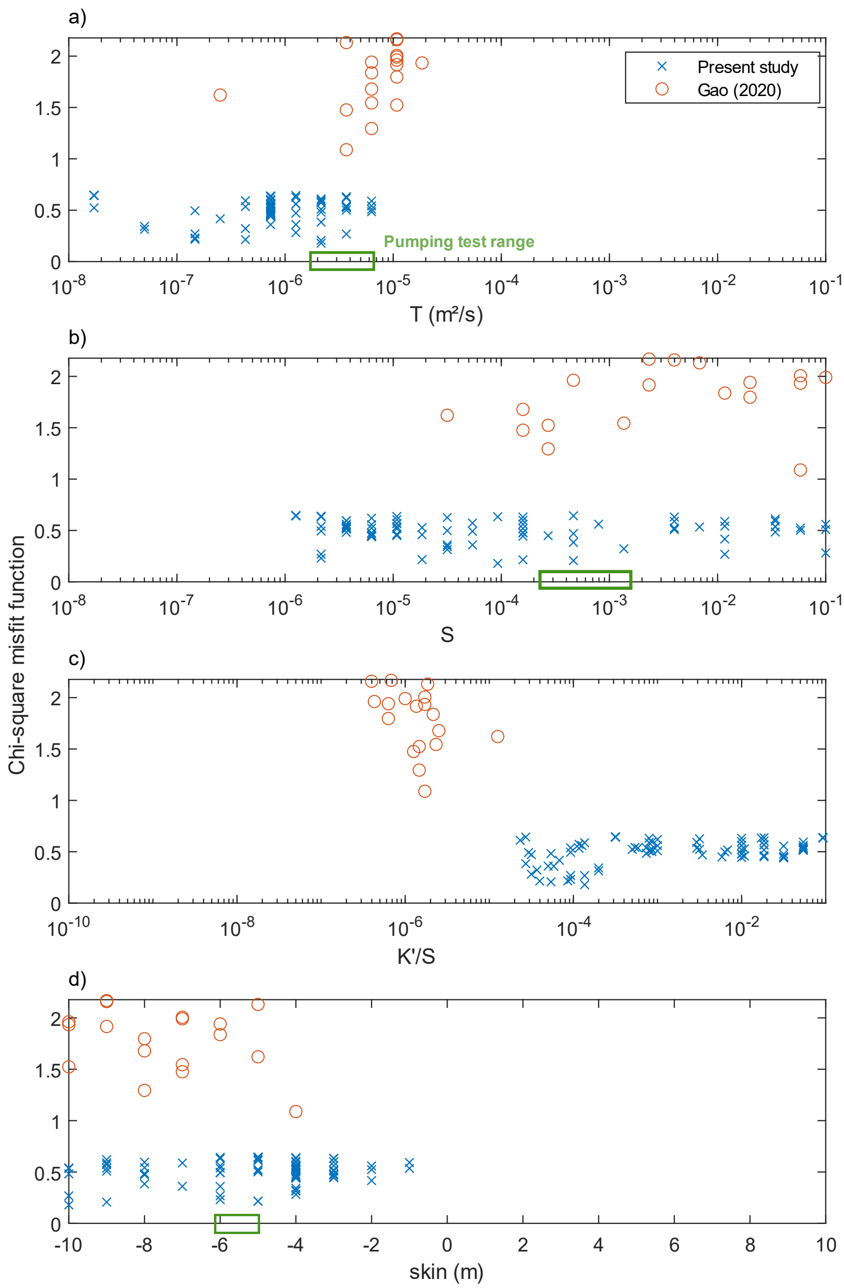

Figure A1: Comparison of misfit function for the present model and the one of Gao et al. (2020) for the Cambodian case study. Only the first hundred best-fit were plotted.